

A Novel & Effective Detection of Alzheimer's Disease using Extremely Randomized Trees Models

¹Mrs. Bingi Manorama Devi, ²Dr. D. Ganesh,

¹ Research Scholar, Department of CSE, Mohan Babu University (Erstwhile Sree Vidyanikethan Engineering College (Autonomous)), Tirupati, Andhra Pradesh, India,
bingimanorama@gmail.com

² Associate Professor of CSE, Mohan Babu University (Erstwhile Sree Vidyanikethan Engineering College (Autonomous)), Tirupati, Andhra Pradesh, India,
dgani05@gmail.com

3

Article History:

Received: 10-11-2024

Revised: 15-12-2024

Accepted: 19-01-2025

Abstract:

Alzheimer's disease (AD) is a chronic and irreversible brain disease without adequate treatment. However, currently, available drugs can slow the progression of the condition. As a result, detecting Alzheimer's disease early is essential to avoiding and limiting the disease's progression. The primary purpose of this research is to establish a comprehensive framework for the early identification of Alzheimer's disease and the medical classification of the disease's various stages. Alzheimer's disease is classified into two stages. The proposed work employed multiple machine learning (ML) approaches such as Gradient boost (GB), Decision Tree (DT), Support Vector Machine (SVM), and Extra tree algorithm (ETA) to diagnose and classify Alzheimer's disease earlier using the Open Access Series of Imaging Studies (OASIS) dataset, with the ETA classifier achieving significant performance and result. The ETA classifier, in particular, outperformed the others regarding total classification performance. The proposed ETA achieves an accuracy of 0.88, precision of 0.93, recall of 0.85, and f1-score of 0.89. The machine learning (ML) technique that we have selected to apply for Alzheimer's disease detection is the Extremely Randomised Trees (extra trees) algorithm. This was a conscious decision on our side. We may classify AD with high accuracy using machine learning methods.

Keywords: Alzheimer's disease; Gradient boosting, machine learning; dementia, Extra tree

1. Introduction

In the current era, dementia is no longer considered a unique disease. It is a broad term for symptoms caused by a decline in memory or other thinking skills severe enough to impair a person's ability to do daily tasks. Alzheimer's disease or another type of dementia can induce these symptoms. Alzheimer's disease is responsible for most cases (60-80%). Vascular dementia is the second most common type of dementia after Alzheimer's disease, which is the primary cause of dementia. However, dementia symptoms can also be caused by several other disorders, some of which are treatable and reversible, such as thyroid problems or vitamin deficiencies. Alzheimer's disease (AD) is a type of dementia having no specific medication and ranks sixth primary death cause in the United States of America [1, 2]. Gradual atrophy of the cerebral cortex characterizes this, developing

cognitive difficulties and memory loss [3]. New technology has enabled the use of computer-assisted algorithms in hospitals, potentially increasing the accuracy and speed of diagnosis. Because of recent developments in the healthcare sector, which have produced powerful tools for collecting and retrieving usable neuroimaging data to monitor neurodegeneration, there is a lot of excitement about using pictures for diagnosis and prognosis. One area where computer algorithms may produce more accurate findings than medical practitioners (for example, radiologists) is AD detection. This ailment first touches memory function, then gradually limits all cognitive tasks, eventually leading to death. Patients with Alzheimer's disease risk becoming disoriented and forgetting how to do ordinary tasks. They can even fail to recognize their own family. Alzheimer's disease and its many stages are difficult to diagnose since symptoms of the disease can be found in the brains of old persons who do not have the disease.

Alzheimer's disease is diagnosed in medical practice utilizing information obtained from a lengthy conversation with a patient's family members who have the disease. In 2018, they expected dementia to affect 35.6 million individuals over 60 worldwide, including 310,000 in Australia. 2050 expect this amount to (almost) triple, bringing the total number of people in the world to 201 million. In 2018, dementia killed 9586 people, making it the country's second-biggest cause of death [4]. Alzheimer's disease (AD) accounts for 60% to 80% of all dementia cases [5, 6]. Even though several therapeutic options have been examined to reduce or stop the progression of the disease [7], very little evidence of efficacy has been found. People diagnosed early are more likely to benefit from supportive therapy, which allows them to spend more time at home and reduces their chances of being hospitalized [8, 9]. Job-specific properties [10, 11] are extracted from images to train supervised models [12]. They need human workers to extract these features, which typically require much work, time, and financial investment. As a result, it is the most challenging problem for data scientists to overcome. On the other hand, deep learning algorithms have advanced to the point where they can now extract features from visual data without human interaction.

The purpose of this paper is to develop an automated model for Alzheimer's disease patients using machine learning (ML) approaches like DT, GB, ETA, and SVM, The classification is based on MRI patient images of the OASIS repository. Also, the proposed classifier reaches 88.21% accuracy, as related to the other works stated in the literature. There are no easily accessible articles that employ ETA to detect MRI-associated Alzheimer's disease (AD).

2. Related work

In this section, AD has been extensively researched and connected to a wide range of difficulties and challenges. On the other hand, there have recently been numerous attempts to use MRI data to diagnose. Here are some examples of work from linked literature:

In [13], the authors constructed a new technique for predicting the progression of mild cognitive impairment (MCI) using MRI. The initial step for the researchers was to apply semi-supervised learning to generate MRI biomarker progression. They next employed supervised learning to connect this biomarker to the subjects' ages and cognitive skills. They eventually decided to make their findings public. They list some unique elements uncovered by various biomarker learning approaches below 1) MRI biomarker development using semi-supervised learning against more

standard supervised methods; 2) MRI biomarker development using a semi-supervised learning strategy. To avoid potential AD, they removed aging effects from the MRI data before classifier training, and feature selection was performed on AD subjects. According to the study's findings, the proposed method may be nominal for early AD detection and for MRI in predicting whether MCI will develop into AD.

In [14], the authors described a computer-aided diagnostic (CAD) system for MRI brain imaging. They would build the system using Eigen brains and machine learning, with two goals in mind: reliably recognizing Alzheimer's disease patients and identifying AD-related brain areas. To begin, 3D volumetric data is subjected to the maximum inter-class variance (ICV) to choose essential slices for subsequent analysis. The following step is for each participant to create an eigenbrain set. The most critical eigenbrain, the MIE, was discovered using Welch's t-test, also known as the WTT. Finally, different kernels were employed in kernel support vector computers to forecast Alzheimer's disease patients correctly. Particle swarm optimization was used to train these machines. We focused on MIE coefficients with values greater than 0.98 quantiles to determine the discriminant areas that discriminate AD from NC. The study's findings revealed that the proposed method might predict AD patients with the same accuracy as existing methods.

In [15], the authors utilized mathematical models to discover potential brain locations associated with Alzheimer's disease. Twenty patients had Alzheimer's disease, with the remaining 13 being healthy controls. To begin, they built the brain's structural network using a technique known as diffusion tensor imaging, or DTI. Unlike graph theory, the 2hop-connectivity measure employs higher-order data within the network topology. To accomplish this goal, the authors devised a novel method called 2hopRWR, an algorithm for measuring two-hop connections. The global feature score (GFS) is an innovative approach for the link evaluating which brain regions to Alzheimer's disease (AD). The GFS was designed to provide an answer to this question. This score was derived by combining five distinct local features: degree centrality, closeness centrality, maximal clique number, and 2hop connectivity. Finally, a canonical correlation analysis revealed a high link between the GFS MMSE and MoCA scale findings.

In [16], the authors comprised three key contributions to these constraints. They began by thoroughly reviewing existing research. They found four fundamental techniques, which are as follows: There are four categories of CNNs such as 2D slice-level, 3D patch-level, ROI-based, and 3D subject-level, respectively. Furthermore, they discovered that more than half of the articles reviewed could have been impacted by data leaks, leading to accusations of biased performance. Our second contribution to the field improved our open-source method for diagnosing Alzheimer's disease using CNN and T1-weighted MRI. A modular set of deep learning-specific picture preparation methods, classification systems, and assessment procedures is supplied in addition to pre-existing tools for automatically transforming data. Finally, they tested the strategy by carefully examining numerous CNN design backgrounds.

In [17], the author aimed to explore if multi-parameter structural MRI features were employed as a meaningful biomarker for distinguishing between vasculovascular disease and Alzheimer's disease. Methods: Between June 2013 and July 2019, 93 people participated in this study. All of them were diagnosed with Alzheimer's disease or vasculocortical dementia, verified by two chief physicians.

The AccuBrain system could get multi-parameter volumetric measurements from various brain regions using automated brain tissue segmentation. To minimize dimensionality, they explored 62 structural MRI biomarkers to find features that differed significantly between VaD and AD. They did this to understand the relationship between the two illnesses better. However, LASSO is employed in creating feature sets and other methods. They employed the feature collection using SVM. To determine whether one classification model is superior to another in VAD and AD, a comparison analysis using several machine learning algorithms was performed and used for the study. They did this to ensure that the model's performance was evaluated objectively.

In [18], the authors described a method for detecting images that employs an effective transfer learning strategy by fine-tuning AlexNet, a pre-trained neural network. The network's settings constructed this system. They did this to aid in the system's development. The construction uses Grey, White, and Cerebral Spinal Fluid images. The suggested system's performance is assessed and evaluated using data from OASIS. The system performed well for non-segmented picture multi-class classification, with an overall accuracy of 92.85%. The system also yielded positive results.

In [19], the authors described T1-weighted MRI, FDG-PET, and regional cerebral blood flow single-photon emission computed tomography (CF-SPECT) in AD subjects. Twenty patients with intermediate Alzheimer's disease and 18 healthy older controls had T1-MRI, FDG-PET, and rCBF-SPECT scans. They analyzed images as part of the experiment to generate SVM-based diagnostic accuracy indices. Researchers combined data from the entire brain with the results of the leave-one-out cross-validation procedure. PET and SPECT measurements had comparable precision and accuracy. The accuracy of PET and SPECT was higher than that of T1-MRI data analysis, which had an AUC of 0.67. PET accuracy varied between 68 and 71%, while SPECT accuracy ranged between 68 and 74%.

3. Materials and Methods

Early Alzheimer's identification is crucial for decreasing the disease's progression and preventing its onset. The proposed framework detects Alzheimer's disease and acts as a classification system for the disease's various stages. The following sections will detail the proposed framework's workflow, preparation algorithms, and medical image classification methods. In diagrammatic form, Figure 1 demonstrates the classification of medical images.

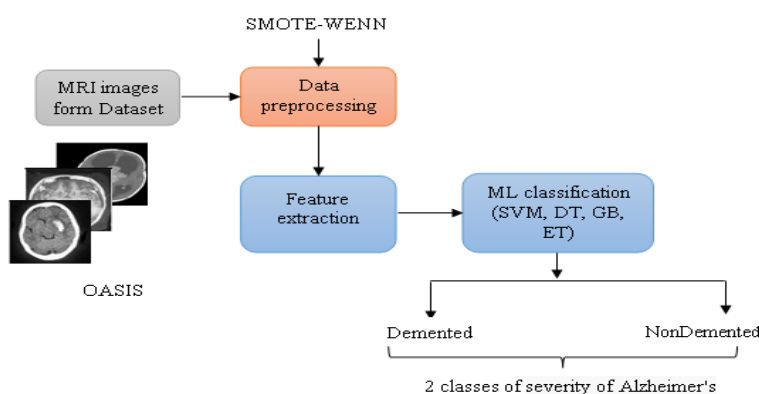


Figure 1: Overview of the proposed framework

3.1 Machine Learning Approach:

The OASIS dataset's cross-sectional MRI data and longitudinal data are the two forms of information included in the dataset collection that was just established here. We produced the resulting data set utilizing information from 150 people aged 60 to 96. All participants were scanned simultaneously, and every single subject was right-handed. During the preliminary visits, 72 participants were diagnosed as not suffering from dementia, while 64 patients were classified as suffering from dementia. However, during the subsequent visits, all subjects were diagnosed with dementia. The following criteria and indicators are used in the evaluation process.

Data Acquisition (Datasets):

The data comes from MRI scans in the OASIS dataset, which may be found at <https://www.oasis-brains.org>. The Open Access to Neuroimaging Datasets in Science (OASIS) Initiative intends to provide scientific researchers with open access to brain neuroimaging datasets [20]. Collecting and freely disseminating neuroimaging datasets will enable and aid future findings and clinical neuroscience like Alzheimer's Disease Neuroimaging Initiative (ADNI) collect and disseminate data. This study reported T1-weighted MRI data from OASIS participants who were either diagnosed with Alzheimer's dementia or did not have the disease.

Clinical Dementia Rating (CDR)

The six domains of cognitive and functional performance associated with Alzheimer's disease and other dementias include memory, orientation, judgment and problem-solving, home and hobbies, community affairs, and personal care. The seventh category is personal care. The CDR is a five-point scale used to classify these various groups. A semi-structured interview with the patient and a credible informant or collateral source (for example, a member of the patient's family) is used to collect the information needed to generate each rating. Table 1 summarises the findings of this interview.

Table 1: Clinical Dementia Rating

Score	Description
0	Normal
0.5	Very Mild Dementia
1	Mild Dementia
2	Moderate Dementia
3	Severe Dementia

The CDR table's descriptive anchors help the physician to assign appropriate ratings based on interview data and clinical judgment. A method can generate an overall CDR score and scores for each domain. This score is vital for characterizing and tracking a patient's level of impairment and dementia as follows: Furthermore, the OASIS-1 dataset had predictor variables types that will be defined in the following sections.

Socio-Demographic Predictor Variables

Numerous OASIS-1 dataset variables provided patient sociodemographic data. They list the variables in Table 2 below.

Table 2:Socio-Demographic Predictor Variables

Variable	value	Description
Gender	0	Female
	1	Male
Age	(18, 96)	-
Education	1	High school
	2	HS Graduate
	3	Some College
	4	College Graduate
	5	Beyond College
Socioeconomic Status (SES)	1	lower
	2	lower middle
	3	middle
	4	upper middle
	5	upper

The CDR table's descriptive anchors help the attending physician to allocate appropriate grades with consultation statistics and medical judgment. There is a method for determining the total score of the CDR in addition to the ratings for each domain. In the following ways, this score can be used to characterize and record a patient's level of impairment and dementia: The OASIS-1 dataset had three categories of predictor variables: demographic, clinical, and imaging predictor variables. In the following paragraphs, definitions for each of these variable categories will be presented.

Clinical Predictor Variables, Non-Imagery Data:

We could also employ other clinical prognostic markers that did not entail imagery omitted from the model since three of the four variables (excluding the MMSE) required imagery. The definitions for these variables will be supplied in the following text.

Minimental State Examination (MMSE). This contains a thirty-question examination that is useful and reliable for dementia diagnosis [21]. We completed the variables at a rate of 56% (235 out of

416). The median was used to fill in the missing values in the data. It included the MMSE in a model that did not consider imaging.

Atlas scaling factor (ASF): (0.88–1.56) (observed). This scaling feature is used to assess estimated total intracranial volume (eTIV) data [22].

Estimated total intracranial volume (eTIV): (1132–1992) mm³ [23]. This calculates the volume of the brain contained within the skull. This variable was complete to the letter (416 out of 416).

Normalized whole brain volume (nWBV): (0.64–0.90) mg (observed). This delivers brain volume estimation.

Preprocessing Step:

The classifications in the obtained dataset are not evenly distributed. To circumvent this issue, we resample using two sampling approaches. Undersampling is the removal of examples from an overrepresented class, whereas oversampling is the addition of more cases to an already adequately represented class. Local imbalance and spatial sparsity are two characteristics associated with sample distribution at the neighbourhood level. Taking these two aspects into consideration, the HVDM distance incorporates the weight constants:

$$d_W^{IR,m}(x_1, x_2) = \begin{cases} e^{(IR^+)^m} \cdot d_{HVDM}(x_1, x_2), & \text{if } x_2 \text{ is positive} \\ e^{(IR^-)^m} \cdot d_{HVDM}(x_1, x_2), & \text{if } x_2 \text{ is negative} \end{cases} \quad (1)$$

where x_1 denotes seed and x_2 denotes candidate for the closest neighbour. The imbalance ratio, abbreviated as IR. Similarly, the weight constants are signified by the symbols f^+ and f^- :

$$f^+(IR, m) = e^{(IR^+)^m}, \quad (2)$$

$$f^-(IR, m) = e^{(IR^-)^m}, \quad (3)$$

Local imbalance:

A global imbalance ratio, represented by IR, gives a rough depiction of the degree of local imbalance. When the quantity of characteristics m is held constant, the weight constants fulfil the aforementioned criteria since $IR^+ > IR$ and the exponential function expands in a steady manner.

$$f^+(IR, m) < f^-(IR, m)$$

Algorithm 1: SMOTE-WENN

Input: T_r , the training set; p , the nearest neighbors in SMOTE; k , the no. of nearest neighbors in data cleaning methods.

Output: New_T_r , the training set after using SMOTE-WENN

Divide into positive and negative subsets; $T_r = Pos \cup Neg$;

Oversample the minority class using SMOTE to balance class distribution;

$New_Pos \leftarrow SMOTE(Pos, p)$ and

$$|New_Pos| = |Neg|;$$

$$New_Tr \leftarrow New_Pos \cup Neg$$

for $x \in New_Tr$ **do**

Compare weighted distances according to (3)

end

Remove noisy examples using ENN based on the weighted distances:

$$New_Tr_r \leftarrow ENN(New_Tr_r, d_w, k)$$

Feature extraction:

We divided the 416 observations into 208 slices, each of which comprised 176 voxels by 176 voxels. The analysis used 51 of these slices, ranging from 78 to 128. These slices were recovered from the original format and placed in a new location as.png files with a single channel (gray-scale). We replicated every image with its own set of corresponding classification labels. The images were given a random transformation after being padded with three voxels on all sides as part of the modeling process. There were only 20,800 MRI images, as opposed to 51times 416, or 21,216. Even without accounting for the one-of-a-kind (and potentially infinite) variations, the total number of voxels in the photos exceeds 640 million.

Classification:

This paper used four ML approaches to classify Alzheimer's disease.

Decision Tree Classifier:

This dataset splits depending on a given constraint to optimize data separation and then displays it as a tree [24]. This approach generates a binary tree with two edges for each node. These edges determine the most relevant category and numerical features to split based on acceptable impurity criteria. Use the Gini and Entropy impureness indices for decision tree categorization. Gini represents impurity.

$$\sum_{i=1}^c f_i(1 - f_i) \tag{4}$$

Where n denotes labels and f_i denotes label frequency.

$$\sum_{i=1}^c -f_i \log(f_i) \tag{5}$$

Support Vector Machine Classifier:

Support vector machines are methods for supervised learning that can be used to tackle classification and regression problems. We know these machines as SVMs. The conventional support vector machine (SVM), currently the most widely used binary classification technique, was applied to structural MRI scan pictures for disease prediction. The SVM is a machine learning classifier that uses a vector of predictions to translate it into a higher-dimensional plane. We achieve this by using

two distinct linear or nonlinear kernel functions. The binary classification problem, according to the concept of structural risk minimization [25], involves two classes (+1 or 1), and it is simple to determine from one another in a hyperplane. Using training data, SVMs are supposed to build a discriminating function capable of accurately classifying new samples (m, n). We can use these in conjunction with kernel models to separate data efficiently. As a result, that hyperplane can communicate with a nonlinear decision boundary while defining SVMs using support vectors:

$$f(m) = \text{sign}\left(\sum a_i y_i K(s_i, x)\right) + w_0 \tag{6}$$

Where K is a kernel term and s_i is the support vectors and a_i is a weight constant [26].

Gradient Boosted Tree Ensembles (Gradient Boosting):

In this, the MMSE and socio-demographic data were used to categorize AD. This model improves prediction accuracy by building weaker decision and classification tree models one after the other. We have also known this model as a gradient-boosted machine (GBM). A classification tree model aims to construct a decision tree capable of delivering a classification vote. We accomplish this by dividing the independent variables throughout the model. The Gini impurity or cross-entropy equations (Eq. 7 and 8) [27, 28] are commonly employed to determine such splits. In these equations, k represents the total number of classes, and p_i represents the percentage of total cases that belong to a specific class.

$$\text{Gini impurity} = \sum_{i=1}^k p_i(1 - p_i) \tag{7}$$

$$\text{Cross - entropy} = - \sum_{i=1}^k p_i \log p_i \tag{8}$$

Using these equations, the splitting algorithm makes an aggressive, greedy attempt to establish homogeneity. Pruning keeps the trees from becoming overburdened by restrictive branches, and they show its overview in Figure 2.

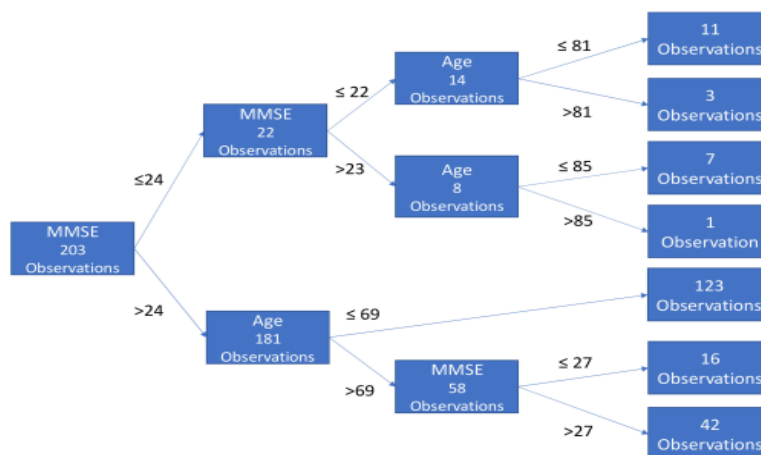


Figure 2: Overview of classification

3.2 Proposed Classification Method: Extra Trees Algorithm (ETA)

The approach gets its name from the randomness with which we generate each DT. The fundamental goal of the endeavor to handle numerically valued features was to lessen the likelihood of the model overfitting to the data. The extra trees algorithm's functionality is based on training a set of binary decision trees (DTs). The accuracy of the ensemble's predictions can be attributed to the fact that each DT should be classified. During the DT training phase, the procedure arbitrarily selects numerous data columns without replacing any of them and will attempt to identify which column best depicts the data. Each column has a distinct feature that goes deeper into a particular aspect of the collected data. We used the Gini index, a derivative of a different scoring approach entirely. We rated the various data sets based on their performance on the Gini index. The Gini index is a value ranging from 0 to 1 that indicates the likelihood of erroneously classifying the data if we choose a classification at random in proportion to what is currently present in the data. This number is a percentage that ranges between 0 and 1. Given these considerations, we aim to discover which category has the lowest Gini index value. When applied to a specific division, the Gini index is defined as follows: $G(A_j) = 1 - \sum_{i=1}^2 \left(\frac{|S_i|}{|S|} \sum_{j=1}^C \left((p_{i,j})^2 \right) \right)$ where S represents the existing data set, S_i represents one dataset, C represents the total classifications, and $p_{i,j}$ represents the proportion of the i -th data subset represented by the j -th classification.

The structure of the tree is then built recursively using the same fundamentals until one of the three conditions is met:

1. All class labels in the node's subset of data are the similar.
2. The node receives fewer rows than a specific limit.
3. Each column of data has only one distinct value.

After a stopping state, we returned the probability distribution and data set class label frequencies. The distribution removes outliers. Thus, we may weigh each ensemble tree's vote. Repeat the process m times to train m trees. In "Algorithm 1," we employ a high-level pseudo code to train a single DT.

Algorithm 1: Procedure of ETA

Input: Training set S .

Output: $E = t_1, \dots, t_m$

1 Function Construct required no.of trees (S, k, m, n)

2 if $|S| \leq n$ **or** all classes in S are constant **then**

3 return class frequencies

4 else

5 A random selection of k (non-constant valued) attributes, $\{a_1, \dots, a_k\}$, from all of the candidate attributes in S is to be made without replacement.

6 Produce k splits, $\{s_1, \dots, s_k\}$

7 Choose s' so that it fulfils the following equation: $\text{Score}(s', S) = \max_{i=1, \dots, k} \text{Score}(s_i, S)$,

8 From s' , split S

9 Consider $t_l = \text{Construct extra tree}(S_l)$ and $t_r = (S_r)$

10 Generate a node N with the split s'

11 end

12 return N

4. Results and Discussion:

In this case, we resolved every classification issue using Windows 10, Python 3.6, and the Scikit-learn module version 0.19.2. We separated participants in this study into two groups: those who had dementia and those who did not. As a result, to validate our proposed solution, we used Anaconda for Python and TensorFlow on a computer with 8 gigabytes of random access memory and a graphics processing unit with Intel HD 6000 1536 megabytes. Due to the small amount of the dataset, 5-fold cross-validation is used.

F1-Score is a prominent measure for assessing the precision of binary classification. The score is calculated using both recall and precision. When computing recall, the denominator includes all similar samples that must be true, while the numerator includes the total number of correct, true outputs. Furthermore, the precision is calculated by dividing the total number of correct outcomes by the number of correct results produced by the classifier. The F1-score should be set to 1 for the best potential results, according to Equation (9).

$$F1 - score = \frac{Recall \times Precision}{Precision + Recall} \times 2 \quad (9)$$

Precision: Because we want to have faith in our forecast, accuracy is highly useful because it shows us what proportion of the values expected to be positive were positive, as shown by Equation (10).

$$Precision = \frac{TP}{TP + FP} \quad (10)$$

Recall: It is also used in binary classification to validate the positive examples found. The true positive rate, also called recall, is used to represent the percentage of people who are infected with a disease. Equation (11) can be used to determine the recall percentage.

$$Recall = \frac{TP}{TP + FN} \quad (11)$$

Accuracy: The term accuracy can be used to calculate the proportion of correct classification of all observations. To establish the precision, equation (12) is used.

$$Accuracy = \frac{TP + TN}{TP + FP + TN + FN} \quad (12)$$

The words True Positive (TP), False Positive (FP), True Negative (TN), and False Negative (FN) have been used to refer to symbols in the equations presented.

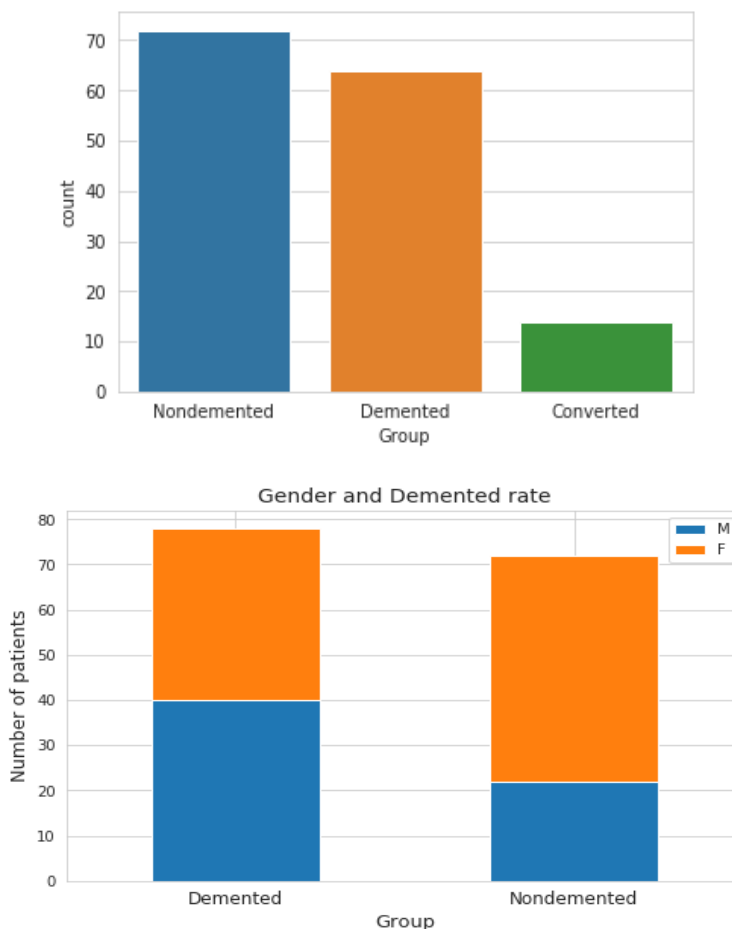


Figure3: Count of patient ID

Table 3: classification for each method in minority class for Accuracy, Precision, Recall, and F1-score

Model	Accuracy	Precision	Recall	F1-score
SVM	0.78	0.87	0.68	0.77
DT	0.79	0.84	0.77	0.80
GB	0.84	0.86	0.83	0.85
Proposed ETA	0.88	0.93	0.85	0.89

Figure 4 depicts the image classifier's performance evaluation. We evaluated the performance using a variety of algorithms. The four algorithms studied and compared were SVM, DT, GB, and ETA.

SVM, DT, GB, and ETA were found to have accuracy values of 0.78, 0.79, 0.84, and 0.88, respectively. Precision levels for ETA range from 0.93 to 0.84, with 0.93 being the highest and 0.84 being the lowest for the DT model. The ETA model has the highest potential recall value of 0.85, while the DT model has the lowest possible value of 0.77. For the f1-score analysis, the SVM, DT, GB, and ETA values were 0.77, 0.80, 0.85, and 0.89, respectively.

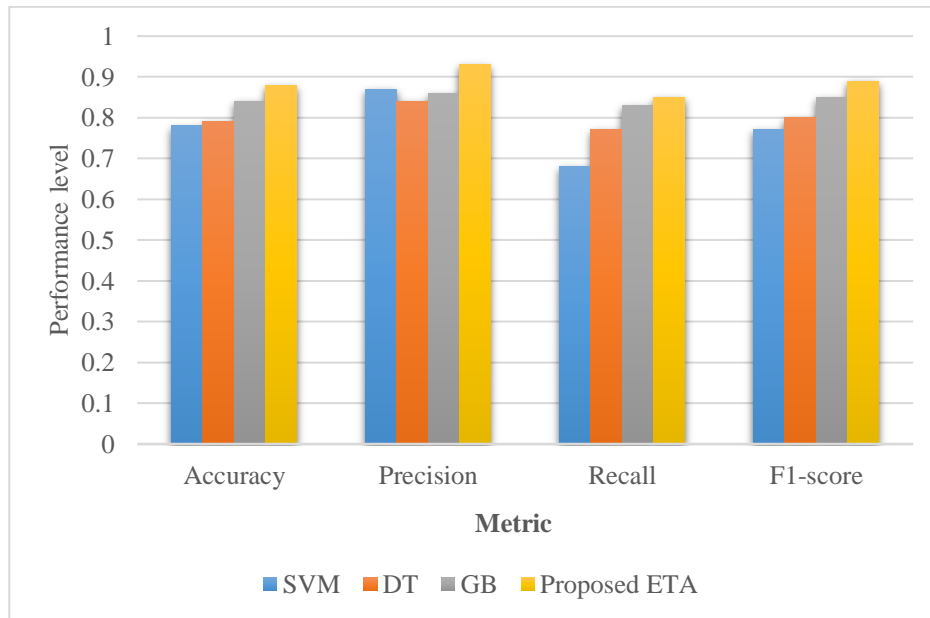


Figure 4: Performance comparison of proposed work and state-of-the-methods for four metrics

When the suggested model is analysed based on accuracy and loss for number of epochs, the accuracy improves but the loss improves less as depicted in Figures 5(a) and 5(b).

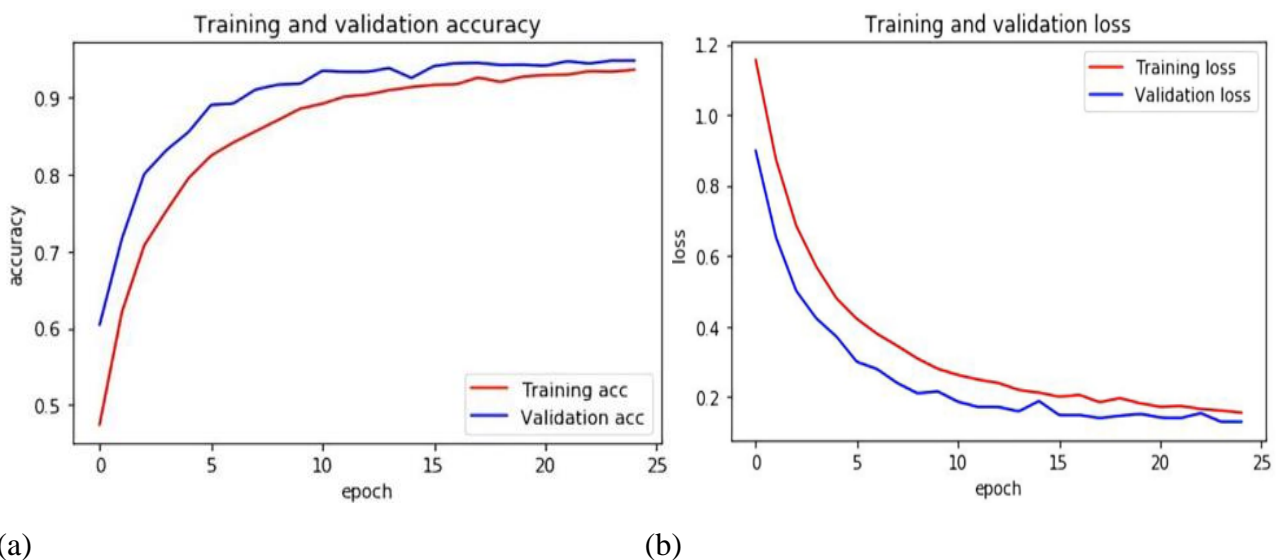


Figure 5: Training and validation accuracy and loss for proposed work

Figure 6 is the receiver operating characteristic (ROC) curve that shows the AUC of our work is 0.99 for all of the 5 folds.

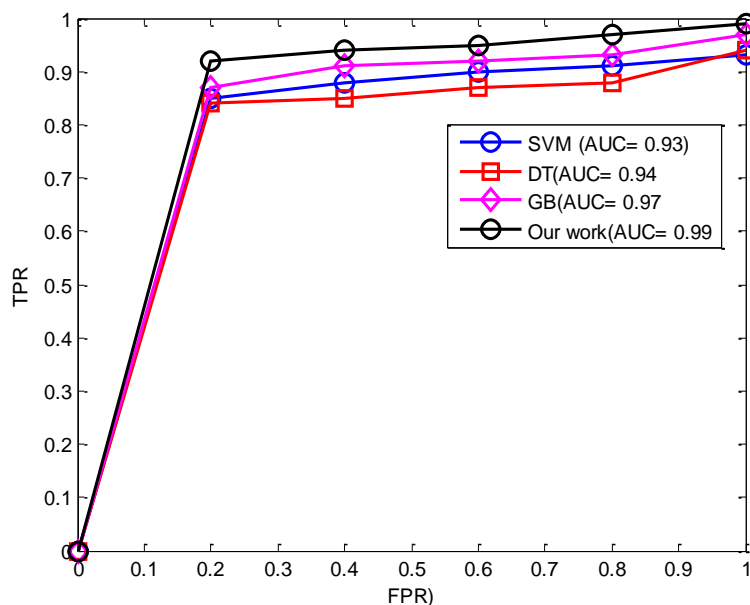


Figure 6: AUC curve for ML approaches

Conclusions:

Using machine learning and data mining techniques to detect and diagnose a wide range of ailments would greatly benefit medicine and healthcare research. The most common myth regarding Alzheimer's disease is that it is a degenerative disorder that cannot be cured and ultimately results in neuronal cell death. Regarding Alzheimer's disease categorization, the machine learning technique has seen tremendous success in the medical sector, and it does not require any handmade feature extraction strategy to accomplish this accomplishment. We propose SMOTE-WENN, a hybrid resampling strategy, as a solution to the problem of restricted sample sizes resulting in imbalanced data classification in this study. SMOTE-WENN can save a significant proportion of both good and bad examples of safe behavior. This exploits the WENN distance scalings for positive and negative candidates whose nearest neighbors are different. The results of the experiments reveal that the proposed designs are appropriate examples of basic structures that minimize the complexity of computational time, memory requirements, and overfitting and provide more efficient time. Furthermore, 2D multi-class AD stage classifications reach highly promising accuracy levels, 93.61%, and 95.17%, respectively.

References:

- [1] Mayeux, R.; Sano, M. Treatment of Alzheimer's disease. *N. Engl. J. Med.* 1999, 341, 1670–1679.
- [2] Alzheimer's Association. Facts and Figures. Available online: <https://www.alz.org/alzheimers-dementia/facts-figures> (accessed on 15 October 2018).
- [3] VanMeter, K.; Hubert, R.J. *Gould's Pathophysiology for the Health Professions*, 6th ed.; Elsevier: St. Louis, MO, USA, 2017.

- [4] A. Krizhevsky, I. Sutskever, and G. E. Hinton, Imagenet classification with deep convolutional neural networks (2012), *Advances in neural information processing systems*, p. 1097-1105.
- [5] H. Greenspan, B. van Ginneken, and R. M. Summers, Guest Editorial Deep Learning in Medical Imaging: Overview and Future Promise of an Exciting New Technique (2016), *IEEE Transactions on Medical Imaging*, vol. 35, no 5, p. 1153–1159.
- [6] Driscoll, I.; Troncoso, J. Asymptomatic Alzheimer’s Disease: A Prodrome or a State of Resilience? *Curr. Alzheimer Res.* 2011, 8, 330–335.
- [7] ThijsKooi, why skin lesions are peanuts and brain tumors a harder nut (2020), *The Gradient*
- [8] A. Gupta, M. Ayhan, and A. Maida, Natural image bases to represent neuroimaging data (2013), *International conference on machine learning*, p. 987–994
- [9] A. Payan and G. Montana, Predicting Alzheimer’s disease: a neuroimaging study with 3D convolutional neural networks (2015), *arXivPrepr. arXiv1502.02506*
- [10] Zhao, Jiayi & Li, Kaixin & Liao, Xiaoyang. (2022). Working status and risk of Alzheimer's disease: A Mendelian randomization study. *Brain and Behavior*. 13. 10.1002/brb3.2834.
- [11] HosseinzadehKasani, Payam & Kim, Jung-Kyeom & Kassani, Peyman & Kim, Yeshin & Kim, Jeong-Ah & Park, Chihyun & Yun, Cheol-Heui & Choi, Sang-Hoon & Lee, Sang-Ah & Lee, Seo-Young & Jang, Jae Won. (2022). A Machine Learning-Based Approach for Classification of Alzheimer’s Disease and its Risk Prediction. *Alzheimer's & Dementia*. 18. 10.1002/alz.064066.
- [12] J. Islam and Y. Zhang, “An ensemble of deep convolutional neural networks for Alzheimer’s disease detection and classification,” <http://arxiv.org/abs/1712.01675>.
- [13] Moradi, Elaheh & Pepe, Antonietta & Gaser, Christian & Huttunen, Heikki & Tohka, Jussi. (2014). Machine learning framework for early MRI-based Alzheimer's conversion prediction in MCI subjects. *NeuroImage*. 104. 10.1016/j.neuroimage.2014.10.002.
- [14] Zhang, Yu-Dong & Dong, Zhengchao & Phillips, Preetha & Wang, Shuihua & Ji, Genlin & Yang, Jiquan & Yuan, Ti-Fei. (2015). Detection of subjects and brain regions related to Alzheimer's disease using 3D MRI scans based on eigenbrain and machine learning. *Frontiers in computational neuroscience*. 9. 66. 10.3389/fncom.2015.00066.
- [15] Wang, Qi & Chen, Siwei & Wang, He & Chen, Luzeng & Sun, Yongan & Yan, Guiying. (2021). Predicting Brain Regions Related to Alzheimer's Disease Based on Global Feature. *Frontiers in Computational Neuroscience*. 15. 10.3389/fncom.2021.659838.
- [16] Wen, Junhao & Thibeau-Sutre, Elina & Diaz-Melo, Mauricio & Samper-Gonzalez, Jorge & Routier, Alexandre & Bottani, Simona & Dormont, Didier & Durrleman, Stanley & Burgos, Ninon & Colliot, Olivier. (2020). Convolutional Neural Networks for Classification of Alzheimer's Disease: Overview and Reproducible Evaluation. *Medical Image Analysis*. 63. 101694. 10.1016/j.media.2020.101694.
- [17] Zheng, Yineng & Guo, Haoming & Zhang, Lijuan & Wu, Jiahui & Li, Qi & Lv, Fajin. (2019). Machine Learning-Based Framework for Differential Diagnosis Between Vascular Dementia

and Alzheimer's Disease Using Structural MRI Features. *Frontiers in Neurology*. 10. 1097. 10.3389/fneur.2019.01097.

- [18] Maqsood, Muazzam&Nazir, Faria& Khan, Umair&Aadil, Farhan& Jamal, Habibullah&Mehmood, Irfan& Song, Oh-Young &Yasir, Somiya. (2019). Transfer Learning Assisted Classification and Detection of Alzheimer's Disease Stages Using 3D MRI Scans. *Sensors*. 19. 2645. 10.3390/s19112645.
- [19] Ferreira, Luiz&Rondina, Jane & Kubo, Rodrigo & Ono, Carla &Leite, Claudia &Smid, Jerusa&Bottino, Cássio&Nitrini, Ricardo &Busatto, Geraldo & Duran, Fabio &Buchpiguel, Carlos. (2017). Support vector machine-based classification of neuroimages in Alzheimer's disease: Direct comparison of FDG-PET, rCBF-SPECT and MRI data acquired from the same individuals. *Revista Brasileira de Psiquiatria*. 40. 10.1590/1516-4446-2016-2083.
- [20] HodaBadr, T.A.R., Carmack, C.L., Kashy, D.A., Cristofanilli, M.: 基因的改变NIH public access. *Bone* 23(1), 1–7 (2011). <https://doi.org/10.1161/circulationaha.110.956839>.
- [21] Morris, J.C. The Clinical Dementia Rating (CDR): Current version and scoring rules. *Neurology* 1993, 43, 2412–2414.
- [22] Open Access Series of Imaging Studies (OASIS). Available online: <http://www.oasis-brains.org/>.
- [23] Buckner, R.L.; Head, D.; Parker, J.; Fotenos, A.F.; Marcus, D.; Morris, J.C.; Snyder, A.Z. A unified approach for morphometric and functional data analysis in young, old, and demented adults using automated atlas-based head size normalization: Reliability and validation against manual measurement of total intracranial volume. *Neuroimage* 2004, 23, 724–738.
- [24] Dreiseitl, S., Ohno-Machado, L.: Logistic regression and artificial neural network classification models: a methodology review. *J. Biomed. Inf.* 35(5–6), 352–359 (2002). [https://doi.org/10.1016/S1532-0464\(03\)00034-0](https://doi.org/10.1016/S1532-0464(03)00034-0).
- [25] Maroco, J., Silva, D., Rodrigues, A., Guerreiro, M., Santana, I., de Mendonça, A.: Data mining methods in the prediction of Dementia: a real-data comparison of the accuracy, sensitivity and specificity of linear discriminant analysis, logistic regression, neural networks, support vector machines, classification trees and random forests. *BMC Res. Notes* 4(1), 1–14 (2011).
- [26] Savio, A.: Supervised classification using deformation-based features for Alzheimer's disease detection on the OASIS cross-sectional database. *Front. Artif. Intell. Appl.* 243, 2191–2200 (2012).
- [27] Cao, J.; Su, Z.; Yu, L.; Chang, D.; Li, X.; Ma, Z. Softmax Cross Entropy Loss with Unbiased Decision Boundary for Image Classification. In *Proceedings of the 2018 Chinese Automation Congress (CAC)*, Xi'an, China, 30 November–2 December 2018; p. 2028.
- [28] Zhang, Y.; Yao, J. Gini objective functions for three-way classifications. *Int. J. Approx. Reason.* 2017, 81, 103–114.